

**Table 1** Multiple sclerosis-linked molecules of the KeyMolnet library

KeyMolnet ID	KeyMolnet symbol	Description
KMMC:04422	2,3cnPDE	2',3'-cyclic nucleotide 3'-phosphodiesterase
KMMC:04421	aBcrystallin	Alpha crystallin B chain
KMMC:01024	ADAM17	A disintegrin and metalloproteinase 17
KMMC:04753	AMPA	AMPA-type glutamate receptor
KMMC:00019	APP	Amyloid beta A4 protein
KMMC:07424	AQP4	Aquaporin 4
KMMC:06672	b-arrestin1	Beta-arrestin 1
KMMC:04017	BAFF	B-cell activating factor
KMMC:00868	Bcl-2	B-cell lymphoma 2
KMMC:00728	Ca	Calcium ion
KMMC:00605	caspase-1	Caspase-1
KMMC:00429	CCL2	Chemokine (C-C motif) ligand 2
KMMC:00425	CCL3	Chemokine (C-C motif) ligand 3
KMMC:00424	CCL5	Chemokine (C-C motif) ligand 5
KMMC:00450	CCR1	Chemokine (C-C motif) receptor 1
KMMC:00454	CCR5	Chemokine (C-C motif) receptor 5
KMMC:03088	CD28	T-cell-specific surface glycoprotein CD28
KMMC:00530	CD80	T-lymphocyte activation antigen CD80
KMMC:03089	CTLA-4	Cytotoxic T-lymphocyte protein 4
KMMC:00418	CXCL10	Chemokine (C-X-C motif) ligand 10
KMMC:00447	CXCR3	Chemokine (C-X-C motif) receptor 3
KMMC:00271	ERa	Estrogen receptor alpha
KMMC:00362	FGF-2	Fibroblast growth factor 2
KMMC:04423	GFAP	Glial fibrillary acidic protein
KMMC:01120	Glu	Glutamic acid
KMMC:00396	glucocorticoid	Glucocorticoid
KMMC:03232	hH1R	Histamine H1 receptor
KMMC:00344	HLA class II	HLA class II histocompatibility antigen
KMMC:09224	HLA-C5	HLA-C5
KMMC:09221	HLA-DQA1*0102	HLA-DQA1*0102
KMMC:06358	HLA-DQA1*0301	HLA-DQA1*0301
KMMC:06359	HLA-DQB1*0302	HLA-DQB1*0302
KMMC:09222	HLA-DQB1*0602	HLA-DQB1*0602
KMMC:06309	HLA-DRB1	HLA-DRB1
KMMC:06315	HLA-DRB1*0301	HLA-DRB1*0301
KMMC:09223	HLA-DRB1*0405	HLA-DRB1*0405
KMMC:09191	HLA-DRB1*11	HLA-DRB1*11
KMMC:07762	HLA-DRB1*15	HLA-DRB1*15
KMMC:06903	HLA-DRB1*1501	HLA-DRB1*1501
KMMC:07763	HLA-DRB1*1503	HLA-DRB1*1503
KMMC:09220	HLA-DRB5*0101	HLA-DRB5*0101
KMMC:04418	HSP105	Heat-shock protein 105 kDa
KMMC:00526	IFNb	Interferon beta
KMMC:00404	IFNg	Interferon gamma
KMMC:00292	IGF1	Insulin-like growth factor 1
KMMC:03611	IgG	Immunoglobulin G
KMMC:00402	IL-10	Interleukin-10
KMMC:03248	IL-12	Interleukin-12
KMMC:04266	IL-12Rb2	Interleukin-12 receptor beta-2 chain
KMMC:03129	IL-17	Interleukin-17
KMMC:03383	IL-18	Interleukin-18
KMMC:00521	IL-1b	Interleukin-1 beta
KMMC:00296	IL-2	Interleukin-2
KMMC:06578	IL-23	Interleukin-23
KMMC:00533	IL-2Rac	Interleukin-2 receptor alpha chain
KMMC:00400	IL-4	Interleukin-4
KMMC:03255	IL-5	Interleukin-5

KeyMolnet ID	KeyMolnet symbol	Description
KMMC:00108	IL-6	Interleukin-6
KMMC:03257	IL-7Rac	Interleukin-7 receptor alpha chain
KMMC:00523	IL-9	Interleukin-9
KMMC:00555	iNOS	Inducible nitric oxide synthase
KMMC:00982	int-a4/b1	Integrin alpha-4/beta-1
KMMC:00968	int-aM	Integrin alpha-M
KMMC:00970	int-aX	Integrin alpha-X
KMMC:04094	MBP	Myelin basic protein
KMMC:06533	mGluR	Metabotropic glutamate receptor
KMMC:04420	MOG	Myelin-oligodendrocyte glycoprotein
KMMC:04419	MPLP	Myelin proteolipid protein
KMMC:03210	N-VDCC	Voltage dependent N-type calcium channel
KMMC:04712	NCAM	Neural cell adhesion molecule
KMMC:06537	NCE	Na(+)-Ca <sup>2+</sup> exchanger
KMMC:05576	NeuroF	Neurofilament protein
KMMC:09225	neurofascin	Neurofascin
KMMC:05903	NF-H	Neurofilament triplet H protein
KMMC:05904	NF-L	Neurofilament triplet L protein
KMMC:03785	NMDAR	N-methyl-D-aspartate receptor
KMMC:07764	NMDAR1	N-methyl-D-aspartate receptor subunit NR1
KMMC:07765	NMDAR2C	N-methyl D-aspartate receptor subtype 2C
KMMC:07766	NMDAR3A	N-methyl-D-aspartate receptor subtype NR3A
KMMC:02064	NO	Nitric oxide
KMMC:07767	Olig-1	Oligodendrocyte transcription factor 1
KMMC:01005	OPN	Osteopontin
KMMC:03073	PDGF	Platelet derived growth factor
KMMC:06225	Sema3A	Semaphorin 3A
KMMC:06229	Sema3F	Semaphorin 3F
KMMC:00111	SMAD3	Mothers against decapentaplegic homolog 3
KMMC:03839	tau	Microtubule-associated protein tau
KMMC:00349	TNFa	Tumor necrosis factor alpha
KMMC:00545	VCAM-1	Vascular cell adhesion protein 1
KMMC:03832	VD	Vitamin D
KMMC:03711	VDR	Vitamin D3 receptor

Table 1 (Continued)

91 multiple sclerosis-linked molecules of the KeyMolnet library are listed in alphabetical order.

analysis. Among 2574 proteins determined with high confidence, the INTERSECT/INTERACT program identified 158, 416 and 236 lesion-specific proteins detected exclusively in AP, CAP and CP, respectively. They found that overproduction of five molecules involved in the coagulation cascade, including tissue factor and protein C inhibitor, plays a central role in molecular events ongoing in CAP. Furthermore, *in vivo* administration of coagulation cascade inhibitors really reduced the clinical severity in EAE, supporting the view that the blockade of the coagulation cascade would be a promising approach for treatment of MS.<sup>43</sup> However, nearly all remaining proteins are uncharacterized in terms of their implications in MS brain lesion development.

We studied molecular networks and pathways of the proteome dataset of Han et al. by using four

different bioinformatics tools for molecular network analysis, such as KEGG, PANTHER, KeyMolnet and IPA.<sup>45</sup> KEGG and PANTHER showed the relevance of extracellular matrix (ECM)-mediated focal adhesion and integrin signaling to CAP and CP proteome. KeyMolnet by the N-points to N-points search disclosed a central role of the complex interaction among diverse cytokine signaling pathways in brain lesion development at all disease stages, as well as a role of integrin signaling in CAP and CP. IPA identified the network constructed with a wide range of ECM components, such as COL1A1, COL1A2, COL6A2, COL6A3, FN1, FBLN2, LAMA1, VTN and HSPG2, as one of the networks highly relevant to CAP proteome. Thus, four distinct tools commonly suggested a role of ECM and integrin signaling in development of chronic

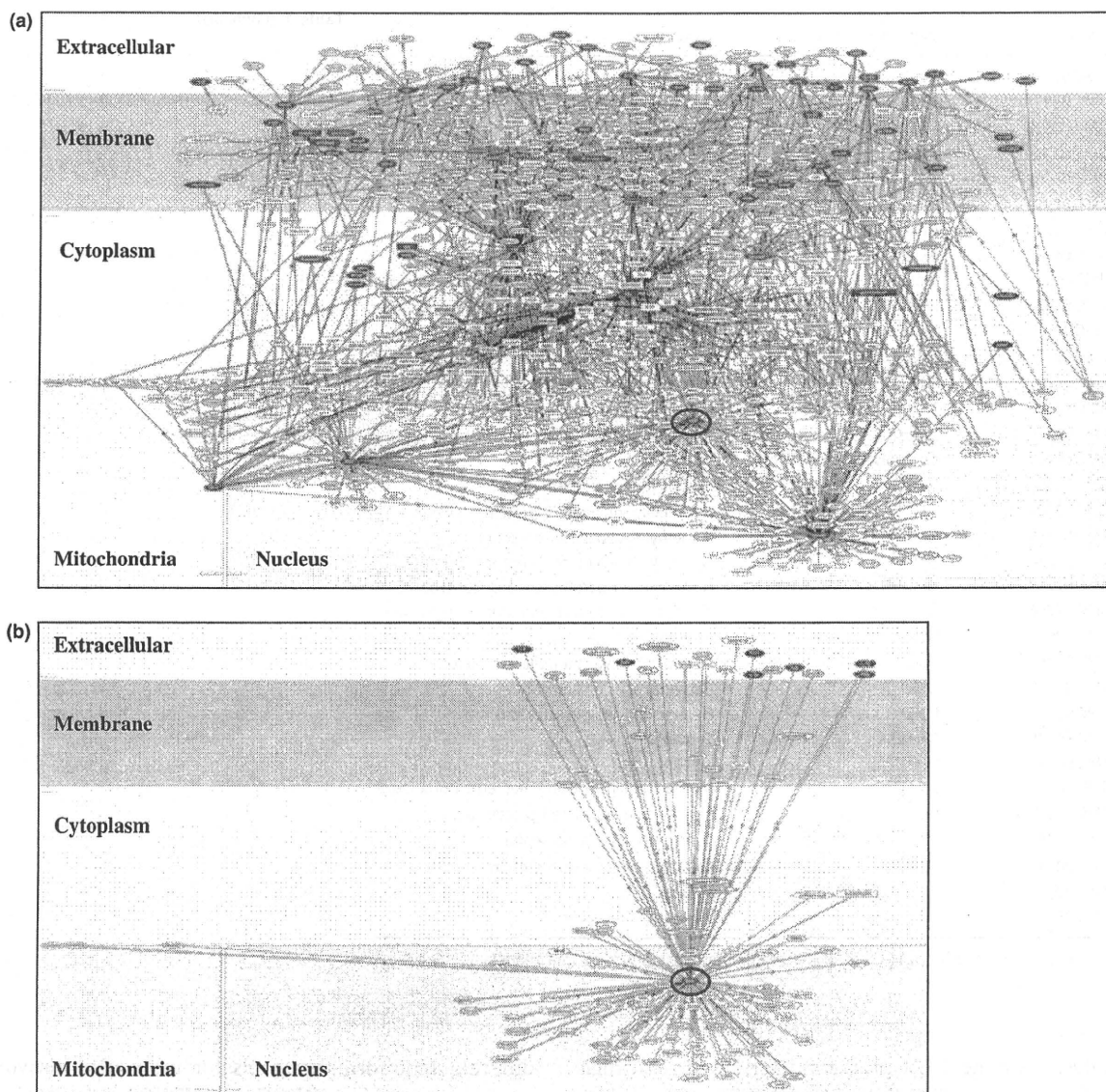


**Figure 2** Molecular network of 91 MS-linked molecules. (a) By importing 91 MS-linked molecules into KeyMolnet, the neighboring search within one path from starting points generates the highly complex molecular network composed of 913 molecules and 1005 molecular relations. (b) The extracted network shows the most significant relationship with transcriptional regulation by vitamin D receptor (VDR) that has direct connections with 118 closely related molecules of the extracted network. VDR is indicated by blue circle. Red nodes represent start point molecules, whereas white nodes show additional molecules extracted automatically from core contents to establish molecular connections. The molecular relation is shown by a solid line with an arrow (direct binding or activation), solid line with an arrow and stop (direct inactivation), solid line without an arrow (complex formation), dash line with an arrow (transcriptional activation), and dash line with an arrow and stop (transcriptional repression). Please refer high resolution figures to URL ([www.my-pharm.ac.jp/~satoj/sub22.html](http://www.my-pharm.ac.jp/~satoj/sub22.html)).

MS lesions, showing that the selective blockade of the interaction between ECM and integrin molecules in brain lesions *in situ* would be a target for therapeutic intervention to terminate ongoing events responsible for the persistence of inflammatory demyelination.

#### KeyMolnet identifies a candidate of molecular targets for MS therapy

The KeyMolnet library includes 91 MS-linked molecules, collected from selected review articles with the highest reliability (Table 1). By importing the list

KeyMolnet ID	KeyMolnet symbol	Description
KMMC:02959	1a,25(OH)2D3	1 alpha, 25-dihydroxyvitamin D3
KMMC:00751	amphiregulin	Amphiregulin
KMMC:03795	ANP	Atrial natriuretic peptide
KMMC:00090	b-catenin	beta-catenin
KMMC:00301	c-Fos	Protooncogene c-fos
KMMC:00183	c-Jun	Protooncogene c-jun
KMMC:00626	c-Myc	Protooncogene c-myc
KMMC:03813	CA-II	Carbonic anhydrase II
KMMC:04105	CalbindinD28K	Vitamin D-dependent calcium-binding protein, avian-type
KMMC:03531	CalbindinD9K	Vitamin D-dependent calcium-binding protein, intestinal
KMMC:00289	caseinK2	Casein kinase 2
KMMC:04195	CaSR	Extracellular calcium-sensing receptor
KMMC:00268	CBP	CREB binding protein
KMMC:00922	CD44	CD44 antigen
KMMC:00136	CDK2	Cyclin dependent kinase 2
KMMC:00135	CDK6	Cyclin dependent kinase 6
KMMC:01008	collagen	Collagen
KMMC:06770	collagenase-I	Type I collagenase
KMMC:04081	CRABP2	Cellular retinoic acid-binding protein II
KMMC:00060	CRT	Calreticulin
KMMC:00401	CXCL8	Chemokine (C-X-C motif) ligand 8 (IL8)
KMMC:00137	cyclinA	Cyclin A
KMMC:00061	cyclinD1	Cyclin D1
KMMC:05926	cyclinD3	Cyclin D3
KMMC:00093	cyclinE	Cyclin E
KMMC:02960	CYP24A1	Cytochrome P450 24A1
KMMC:02958	CYP27B1	Cytochrome P450 27B1
KMMC:04593	CYP3A4	Cytochrome P450 3A4
KMMC:06769	cystatin M	Cystatin M
KMMC:06762	Cytokeratin 13	Keratin, type I cytoskeletal 13
KMMC:06751	Cytokeratin 16	Keratin, type I cytoskeletal 16
KMMC:00053	DHTR	Dihydrotestosterone receptor
KMMC:00928	E-cadherin	E-cadherin
KMMC:00594	ErbB1	Receptor protein-tyrosine kinase erbB-1
KMMC:00068	filamin	Filamin
KMMC:00341	FN1	Fibronectin 1
KMMC:06760	FREAC-1	Forkhead box protein F1
KMMC:06763	G0S2	G0/G1 switch protein 2
KMMC:00617	GM-CSF	Granulocyte macrophage colony stimulating factor
KMMC:06755	Hairless	Hairless protein
KMMC:05978	HOXA10	Homeobox protein Hox-A10
KMMC:06767	HOXB4	Homeobox protein Hox-B4
KMMC:00404	IFNg	Interferon gamma
KMMC:00579	IGF-BP3	Insulin-like growth factor binding protein 3
KMMC:04498	IGF-BP5	Insulin-like growth factor binding protein 5
KMMC:00402	IL-10	Interleukin-10
KMMC:03241	IL-10R	Interleukin-10 receptor
KMMC:03239	IL-10Rac	Interleukin-10 receptor alpha chain
KMMC:03240	IL-10Rbc	Interleukin-10 receptor beta chain
KMMC:03248	IL-12	Interleukin-12
KMMC:03246	IL-12A	Interleukin-12 alpha chain
KMMC:00403	IL-12B	Interleukin-12 beta chain
KMMC:00296	IL-2	Interleukin-2
KMMC:00108	IL-6	Interleukin-6

**Table 2** Molecules constituting the transcriptional regulation by vitamin D receptor network

**Table 2** (Continued)

KeyMolnet ID	KeyMolnet symbol	Description
KMMC:00973	int-b3	Integrin beta-3
KMMC:03747	IVL	Involucrin
KMMC:00629	JunB	Protooncogene jun-B
KMMC:04334	JunD	Protooncogene jun-D
KMMC:06764	KLK10	Kallikrein-10
KMMC:06765	KLK6	Kallikrein-6
KMMC:04635	Mad1	Max dimerization protein 1
KMMC:06757	Metallothionein	Metallothionein
KMMC:06722	MKP-5	MAP kinase phosphatase 5
KMMC:00595	MMP-2	Matrix metalloproteinase 2
KMMC:03104	MMP-3	Matrix metalloproteinase 3
KMMC:00631	MMP-9	Matrix metalloproteinase 9
KMMC:00556	MnSOD	Manganese superoxide dismutase
KMMC:00927	N-cadherin	N-cadherin
KMMC:00074	NCOA1	Nuclear receptor coactivator 1
KMMC:00075	NCOA2	Nuclear receptor coactivator 2
KMMC:00080	NCOA3	Nuclear receptor coactivator 3
KMMC:00282	NCOR1	Nuclear receptor corepressor 1
KMMC:00270	NCOR2	Nuclear receptor corepressor 2
KMMC:00392	NFAT	Nuclear factor of activated T cells
KMMC:00104	NFkB	Nuclear factor kappa B
KMMC:03120	OPG	Osteoprotegerin
KMMC:01005	OPN	Osteopontin
KMMC:00304	osteocalcin	Osteocalcin
KMMC:00100	p21CIP1	Cyclin dependent kinase inhibitor 1
KMMC:00155	p27KIP1	Cyclin dependent kinase inhibitor 1B
KMMC:00195	p300	E1A binding protein p300
KMMC:03204	PLCb1	Phospholipase C beta 1
KMMC:03295	PLCd1	Phospholipase C delta 1
KMMC:00724	PLCg1	Phospholipase C gamma 1
KMMC:04869	plectin1	Plectin 1
KMMC:06772	PMCA1	Plasma membrane calcium-transporting ATPase 1
KMMC:06766	PP1c	Serine/threonine protein phosphatase PP1 catalytic subunit
KMMC:00786	PP2A	Serine/threonine protein phosphatase 2A
KMMC:03442	PPARd	Peroxisome proliferator activated receptor delta
KMMC:03710	PTH	Parathyroid hormone
KMMC:00346	PTHrP	Parathyroid hormone-related protein
KMMC:03115	RANKL	Receptor activator of NFkB ligand
KMMC:04537	RelB	Transcription factor RelB
KMMC:00091	RIP140	Nuclear factor RIP140
KMMC:00383	RXR	Retinoid X receptor
KMMC:06771	SCCA	Squamous cell carcinoma antigen
KMMC:05340	SKIP	Ski-interacting protein
KMMC:04103	SUG1	26S protease regulatory subunit 8
KMMC:05702	TAFII130	Transcription initiation factor TFIID subunit 4
KMMC:06753	TAFII28	Transcription initiation factor TFIID subunit 11
KMMC:06752	TAFII55	Transcription initiation factor TFIID subunit 7
KMMC:04955	TCF-1	T-cell-specific transcription factor 1
KMMC:03075	TCF-4	T-cell-specific transcription factor 4
KMMC:06754	TFIIA	Transcription initiation factor IIA
KMMC:04089	TFIIB	Transcription initiation factor IIB
KMMC:06768	TGase 1	Transglutaminase 1
KMMC:04184	TGFb1	Transforming growth factor beta 1
KMMC:05986	TGFb2	Transforming growth factor beta 2
KMMC:04104	TIF1	Transcription intermediary factor 1
KMMC:00349	TNFa	Tumor necrosis factor alpha

KeyMolnet ID	KeyMolnet symbol	Description
KMMC:00277	TRAP220	Thyroid hormone receptor-associated protein complex component TRAP220
KMMC:06759	TRPV5	TRP vanilloid receptor 5
KMMC:06758	TRPV6	TRP vanilloid receptor 6
KMMC:06756	TRR1	Thioredoxin reductase 1
KMMC:03711	VDR	Vitamin D3 receptor
KMMC:04853	VDUP1	Vitamin D3 up-regulated protein 1
KMMC:06761	ZNF-44	Zinc finger protein 44
KMMC:05147	ZO-1	Tight junction protein ZO-1
KMMC:05811	ZO-2	Tight junction protein ZO-2

Table 2 (Continued)

118 molecules constituting the transcriptional regulation by VDR network are listed in alphabetical order.

of these molecules into KeyMolnet, the neighboring search within one path from starting points generates the highly complex molecular network composed of 913 molecules and 1005 molecular relations (Fig. 2a). The extracted network shows the most significant relationship with transcriptional regulation by vitamin D receptor (VDR) with *P*-value of the score = 4.415E-242. Thus, VDR, a hub that has direct connections with 118 closely related molecules of the extracted network (Fig. 2b, Table 2), serves as one of the most promising molecular target candidates for MS therapy, because the adequate manipulation of the VDR network capable of producing a great impact on the whole network could efficiently disconnect the pathological network of MS. Indeed, vitamin D plays a protective role in MS by activating VDR, a transcription factor that regulates the expression of as many as 500 genes, although the underlying molecular mechanism remains largely unknown.<sup>46</sup>

### Conclusion

MS is a complex disease with remarkable heterogeneity caused by the intricate interplay between various genetic and environmental factors. Recent advances in bioinformatics and systems biology have made major breakthroughs by illustrating the cell-wide map of complex molecular interactions with the aid of the literature-based knowledgebase of molecular pathways. The efficient integration of high-throughput experimental data derived from the disease-affected cells and tissues with underlying molecular networks helps us to characterize the molecular markers and pathways relevant to MS heterogeneity, and promotes us to identify the network-based effective drug targets for personalized therapy of MS.

### Acknowledgements

This work was supported by grants from the Research on Intractable Diseases, the Ministry of Health, Labour and Welfare of Japan (H22-Nanchi-Ippan-136), and the High-Tech Research Center Project, the Ministry of Education, Culture, Sports, Science and Technology (MEXT), Japan (S0801043). The author thanks Dr Takashi Yamamura, Department of Immunology, National Institute of Neurosciences, NCNP for his continuous help with our studies.

### References

1. Sospedra M, Martin R. Immunology of multiple sclerosis. *Annu Rev Immunol.* 2005; **23**: 683–747.
2. Steinman L. A brief history of T<sub>H</sub>17, the first major revision in the T<sub>H</sub>1/T<sub>H</sub>2 hypothesis of T cell-mediated tissue damage. *Nat Med.* 2007; **13**: 139–45.
3. Lucchinetti C, Brück W, Parisi J, Scheithauer B, Rodriguez M, Lassmann H. Heterogeneity of multiple sclerosis lesions: implications for the pathogenesis of demyelination. *Ann Neurol.* 2000; **47**: 707–17.
4. Rudick RA, Lee JC, Simon J, Ransohoff RM, Fisher E. Defining interferon  $\beta$  response status in multiple sclerosis patients. *Ann Neurol.* 2004; **56**: 548–55.
5. International Multiple Sclerosis Genetics Consortium, Hafler DA, Compston A, Sawcer S, Lander ES, Daly MJ, et al. Risk alleles for multiple sclerosis identified by a genomewide study. *N Engl J Med.* 2007; **357**: 851–62.
6. Lock C, Hermans G, Pedotti R, Brendolan A, Schadt E, Garren H, et al. Gene-microarray analysis of multiple sclerosis lesions yields new targets validated in autoimmune encephalomyelitis. *Nature Med.* 2002; **8**: 500–8.
7. Han MH, Hwang SI, Roy DB, Lundgren DH, Price JV, Ousman SS, et al. Proteomic analysis of active multiple sclerosis lesions reveals therapeutic targets. *Nature.* 2008; **451**: 1076–81.

8. Baranzini SE, Mudge J, van Velkinburgh JC, Khankhanian P, Khrebtukova I, Miller NA, et al. Genome, epigenome and RNA sequences of monozygotic twins discordant for multiple sclerosis. *Nature*. 2010; **464**: 1351–6.
9. Viswanathan GA, Seto J, Patil S, Nudelman G, Sealfon SC. Getting started in biological pathway construction and analysis. *PLoS Comput Biol*. 2008; **4**: e16.
10. Kitano H. A robustness-based approach to systems-oriented drug design. *Nat Rev Drug Discov*. 2007; **6**: 202–10.
11. Albert R, Jeong H, Barabasi AL. Error and attack tolerance of complex networks. *Nature*. 2000; **406**: 378–82.
12. Satoh J, Tabunoki H, Arima K. Molecular network analysis suggests aberrant CREB-mediated gene regulation in the Alzheimer disease hippocampus. *Dis Markers*. 2009; **27**: 239–52.
13. MAQC Consortium, Shi L, Reid LH, Jones WD, Shippy R, Warrington JA, et al. The MicroArray Quality Control (MAQC) project shows inter- and intraplatform reproducibility of gene expression measurements. *Nat Biotechnol*. 2006; **24**: 1151–61.
14. Huang DW, Sherman BT, Lempicki RA. Systematic and integrative analysis of large gene lists using DAVID bioinformatics resources. *Nat Protoc*. 2009; **4**: 44–57.
15. Subramanian A, Tamayo P, Mootha VK, Mukherjee S, Ebert BL, Gillette MA, et al. Gene set enrichment analysis: a knowledge-based approach for interpreting genome-wide expression profiles. *Proc Natl Acad Sci USA*. 2005; **102**: 15545–50.
16. Kanehisa M, Goto S, Furumichi M, Tanabe M, Hirakawa M. KEGG for representation and analysis of molecular networks involving diseases and drugs. *Nucleic Acids Res*. 2010; **38**: D355–60.
17. Mi H, Dong Q, Muruganujan A, Gaudet P, Lewis S, Thomas PD. PANTHER version 7: improved phylogenetic trees, orthologs and collaboration with the Gene Ontology Consortium. *Nucleic Acids Res*. 2010; **38**: D204–10.
18. Jensen LJ, Kuhn M, Stark M, Chaffron S, Creevey C, Muller J, et al. STRING 8 – a global view on proteins and their functional interactions in 630 organisms. *Nucleic Acids Res*. 2009; **37**: D412–6.
19. Pospisil P, Iyer LK, Adelstein SJ, Kassis AI. A combined approach to data mining of textual and structured data to identify cancer-related targets. *BMC Bioinformatics*. 2006; **7**: 354.
20. Sato H, Ishida S, Toda K, Matsuda R, Hayashi Y, Shigetaka M, et al. New approaches to mechanism analysis for drug discovery using DNA microarray data combined with KeyMolnet. *Curr Drug Discov Technol*. 2005; **2**: 89–98.
21. Corvol JC, Pelletier D, Henry RG, Caillier SJ, Wang J, Pappas D, et al. Abrogation of T cell quiescence characterizes patients at high risk for multiple sclerosis after the initial neurological event. *Proc Natl Acad Sci USA*. 2008; **105**: 11839–44.
22. Achiron A, Feldman A, Mandel M, Gurevich M. Impaired expression of peripheral blood apoptotic-related gene transcripts in acute multiple sclerosis relapse. *Ann N Y Acad Sci*. 2007; **1107**: 155–67.
23. Gurevich M, Tuller T, Rubinstein U, Or-Bach R, Achiron A. Prediction of acute multiple sclerosis relapses by transcription levels of peripheral blood cells. *BMC Med Genomics*. 2009; **2**: 46.
24. Achiron A, Grotto I, Balicer R, Magalashvili D, Feldman A, Gurevich M. Microarray analysis identifies altered regulation of nuclear receptor family members in the pre-disease state of multiple sclerosis. *Neurobiol Dis*. 2010; **38**: 201–9.
25. Arthur AT, Armati PJ, Bye C; Southern MS Genetics Consortium, Heard RN, Stewart GJ, et al. Genes implicated in multiple sclerosis pathogenesis from consistency of genotyping and expression profiles in relapse and remission. *BMC Med Genet*. 2008; **9**: 17.
26. Brynedal B, Khademi M, Wallström E, Hillert J, Olsson T, Duvefelt K. Gene expression profiling in multiple sclerosis: a disease of the central nervous system, but with relapses triggered in the periphery? *Neurobiol Dis*. 2010; **37**: 613–21.
27. Satoh J, Misawa T, Tabunoki H, Yamamura T. Molecular network analysis of T-cell transcriptome suggests aberrant regulation of gene expression by NF- $\kappa$ B as a biomarker for relapse of multiple sclerosis. *Dis Markers*. 2008; **25**: 27–35.
28. Barnes PJ, Karin M. Nuclear factor- $\kappa$ B. A pivotal transcription factor in chronic inflammatory diseases. *N Engl J Med*. 1997; **336**: 1066–71.
29. Yan J, Greer JM. NF- $\kappa$ B, a potential therapeutic target for the treatment of multiple sclerosis. *CNS Neurol Disord Drug Targets*. 2008; **7**: 536–57.
30. Satoh J, Illes Z, Peterfalvi A, Tabunoki H, Rozsa C, Yamamura T. Aberrant transcriptional regulatory network in T cells of multiple sclerosis. *Neurosci Lett*. 2007; **422**: 30–3.
31. Du C, Liu C, Kang J, Zhao G, Ye Z, Huang S, et al. MicroRNA miR-326 regulates T<sub>H</sub>-17 differentiation and is associated with the pathogenesis of multiple sclerosis. *Nat Immunol*. 2009; **10**: 1252–9.
32. Byun E, Caillier SJ, Montalban X, Villoslada P, Fernández O, Brassat D, et al. Genome-wide pharmacogenomic analysis of the response to interferon beta therapy in multiple sclerosis. *Arch Neurol*. 2008; **65**: 337–44.
33. Comabella M, Lünemann JD, Río J, Sánchez A, López C, Julià E, et al. A type I interferon signature in monocytes is associated with poor response to interferon- $\beta$  in multiple sclerosis. *Brain*. 2009; **132**: 3353–65.
34. Sellebjerg F, Krakauer M, Hesse D, Ryder LP, Alsing I, Jensen PE, et al. Identification of new sensitive biomarkers for the *in vivo* response to interferon- $\beta$  treatment in multiple sclerosis using DNA-array evaluation. *Eur J Neurol*. 2009; **16**: 1291–8.

35. Weinstock-Guttman B, Badgett D, Patrick K, Hartrich L, Santos R, Hall D, et al. Genomic effects of IFN- $\beta$  in multiple sclerosis patients. *J Immunol.* 2003; **171**: 2694–702.
36. Hesse D, Krakauer M, Lund H, Søndergaard HB, Langkilde A, Ryder LP, et al. Breakthrough disease during interferon- $\beta$  therapy in MS: no signs of impaired biological response. *Neurology.* 2010; **74**: 1455–62.
37. Goertsches RH, Hecker M, Koczan D, Serrano-Fernandez P, Moeller S, Thiesen HJ, et al. Long-term genome-wide blood RNA expression profiles yield novel molecular response candidates for IFN- $\beta$ 1b treatment in relapsing remitting MS. *Pharmacogenomics.* 2010; **11**: 147–61.
38. Fernald GH, Knott S, Pachner A, Caillier SJ, Narayan K, Oksenberg JR, et al. Genome-wide network analysis reveals the global properties of IFN- $\beta$  immediate transcriptional effects in humans. *J Immunol.* 2007; **178**: 5076–85.
39. Baranzini SE, Mousavi P, Rio J, Caillier SJ, Stillman A, Villoslada P, et al. Transcription-based prediction of response to IFN $\beta$  using supervised computational methods. *PLoS Biol.* 2005; **3**: e2.
40. Koike F, Satoh J, Miyake S, Yamamoto T, Kawai M, Kikuchi S, et al. Microarray analysis identifies interferon beta-regulated genes in multiple sclerosis. *J Neuroimmunol.* 2003; **139**: 109–18.
41. Satoh J, Nanri Y, Tabunoki H, Yamamura T. Microarray analysis identifies a set of CXCR3 and CCR2 ligand chemokines as early IFNbeta-responsive genes in peripheral blood lymphocytes in vitro: an implication for IFNbeta-related adverse effects in multiple sclerosis. *BMC Neurol.* 2006; **6**: 18.
42. Satoh J, Nakanishi M, Koike F, Miyake S, Yamamoto T, Kawai M, et al. Microarray analysis identifies an aberrant expression of apoptosis and DNA damage-regulatory genes in multiple sclerosis. *Neurobiol Dis.* 2005; **18**: 537–50.
43. Satoh J, Nakanishi M, Koike F, Onoue H, Aranami T, Yamamoto T, et al. T cell gene expression profiling identifies distinct subgroups of Japanese multiple sclerosis patients. *J Neuroimmunol.* 2006; **174**: 108–18.
44. Axtell RC, de Jong BA, Boniface K, van der Voort LF, Bhat R, De Sarno P, et al. T helper type 1 and 17 cells determine efficacy of interferon- $\beta$  in multiple sclerosis and experimental encephalomyelitis. *Nat Med.* 2010; **16**: 406–12.
45. Satoh JI, Tabunoki H, Yamamura T. Molecular network of the comprehensive multiple sclerosis brain-lesion proteome. *Mult Scler.* 2009; **15**: 531–41.
46. Ascherio A, Munger KL, Simon KC. Vitamin D and multiple sclerosis. *Lancet Neurol.* 2010; **9**: 599–612.



*Forum Minireview*

## MicroRNAs and Their Therapeutic Potential for Human Diseases: Aberrant MicroRNA Expression in Alzheimer's Disease Brains

Jun-ichi Satoh<sup>1,\*</sup>

<sup>1</sup>*Department of Bioinformatics and Molecular Neuropathology, Meiji Pharmaceutical University,  
2-522-1 Noshio, Kiyose, Tokyo 204-8588, Japan*

Received May 27, 2010; Accepted June 25, 2010

**Abstract.** MicroRNAs (miRNAs) are a group of small noncoding RNAs that regulate translational repression of multiple target mRNAs. The miRNAs in a whole cell regulate greater than 30% of all protein-coding genes. The vast majority of presently identified miRNAs are expressed in the brain in a spatially and temporally controlled manner. They play a key role in neuronal development, differentiation, and synaptic plasticity. However, at present, the pathological implications of deregulated miRNA expression in neurodegenerative diseases remain largely unknown. This review will briefly summarize recent studies that focus attention on aberrant miRNA expression in Alzheimer's disease brains.

**Keywords:** Alzheimer's disease, bioinformatics, microRNA, neuropathology

### 1. Introduction

MicroRNAs (miRNAs) constitute a class of endogenous small noncoding RNAs conserved through evolution (1). They mediate posttranscriptional regulation of protein-coding genes by binding to the 3' untranslated region (3'UTR) of target mRNAs, leading to translational inhibition or mRNA degradation, depending on the degree of sequence complementarity. The primary miRNAs (pri-miRNAs) are transcribed from the intra- and inter-genetic regions of the genome by RNA polymerase II, followed by processing by the RNase III enzyme Drosha into pre-miRNAs. After nuclear export, they are cleaved by the RNase III enzyme Dicer into mature miRNAs consisting of approximately 22 nucleotides. Finally, a single-stranded miRNA is loaded onto the RNA-induced silencing complex (RISC), where the seed sequence located at positions 2 – 8 from the 5' end of the miRNA plays a pivotal role in binding to the target mRNA. At present, more than 900 human miRNAs have been identified (miRBase Release 15). A single miRNA reduces the production of hundreds of proteins (2). The miRNAs in a whole cell regulate approximately 30% of all protein-coding genes (3). Furthermore, some miRNAs activate

transcription and translation of the targets (4, 5). Thus, by targeting multiple transcripts and affecting expression of numerous proteins, miRNAs play a key role in cellular development, differentiation, proliferation, apoptosis, and metabolism.

Increasing evidence indicates that a battery of miRNAs, expressed in a spatially and temporally controlled manner in the brain, are involved in neuronal development and differentiation (6). miR-134, localized to the synaptodendritic compartment of hippocampal neurons, regulates synaptic plasticity by inhibiting translation of Lim-domain-containing protein kinase 1 (LIMK1) (7). miR-30a-5p, enriched in layer III pyramidal neurons in the human prefrontal cortex, decreases brain-derived neurotrophic factor (BDNF) protein levels (8). Because a single miRNA has a great impact on the expression of numerous downstream mRNA targets, deregulated expression of even a small set of miRNAs in the brain affects diverse cellular signaling pathways essential for neuronal survival and protection against neurodegeneration (9). Importantly, approximately 70% of presently identified miRNAs are expressed in the brain, but the pathological implications of deregulated miRNA expression in neurodegenerative diseases remain largely unknown (10). The present review will briefly summarize recent studies that focus attention on aberrant miRNA expression in the brains of Alzheimer's disease (AD).

\*Corresponding author. satoj@my-pharm.ac.jp  
Published online in J-STAGE on October 9, 2010 (in advance)  
doi: 10.1254/jphs.10R11FM

## 2. Aberrant miRNA expression in AD brains

AD is the most common cause of dementia worldwide, affecting the elderly population, characterized by the hallmark pathology of amyloid- $\beta$  ( $A\beta$ ) deposition and neurofibrillary tangle (NFT) formation in the brain. Although the precise mechanisms underlying neurodegeneration in AD remain mostly unknown, previous studies support a role of the complex interaction between genetic and environmental factors (11). Furthermore, recent studies indicate the cardinal involvement of deregulated miRNA expression in the pathogenesis of AD (Table 1).

By using a nylon membrane-bound DNA array, a previous study identified upregulated expression of miR-9 and miR-128 in the hippocampus of AD brains, although they did not characterize the target mRNAs (12). More recently, the same group showed that the levels of miR-146a expression are elevated in the hippocampus and the superior temporal cortex of AD (13, 14). Importantly, the expression of miR-146a is directly regulated

by nuclear factor-kappa B (NF- $\kappa$ B), and it targets the mRNA of complement factor H (CFH), a negative regulator of the inflammatory response in the brain. They validated upregulation of NF- $\kappa$ B in the neocortex of AD by gel shift assay, suggesting that activation of NF- $\kappa$ B induces miR-146a that amplifies inflammatory neurodegeneration via reducing CFH in AD brains. Recently, the same group revealed the instability of brain-enriched miRNAs that contain a high content of AU and UA dinucleotides (14).

A previous study showed that miR-107 targets the  $\beta$ -site amyloid precursor protein (APP)-cleaving enzyme 1 (BACE1), a rate-limiting enzyme for  $A\beta$  production (15). By analyzing a microarray, miR-107 levels are substantially reduced in the temporal cortex of the patients affected with mild cognitive impairment (MCI) and those with AD (15). These observations suggest that downregulation of miR-107 begins at the very early stage of AD. A different study showed that miR-29 also targets BACE1 (16). By using a microarray containing 328 miRNAs, they identified reduced expression of the miR-

**Table 1.** Aberrant expression of microRNAs in Alzheimer disease (AD) brains

Authors, years, and reference No.	Brains of AD patients	MicroRNAs aberrantly expressed	Upregulation or downregulation	Target mRNAs characterized	Target prediction and validation	Possible pathological implications
Lukiw, 2007 (12)	Hippocampus of 5 AD patients, 5 age-matched controls, and 5 fetal brains	miR-9, miR-128	up	ND	ND	general neuropathology of AD
Lukiw et al., 2008 (13)	Hippocampus and superior temporal lobe of 23 AD patients and 23 age-matched controls	miR-146a	up	CFH	ND; introduction of an anti-miR-146a oligonucleotide	suppression of anti-inflammatory response
Wang et al., 2008 (15)	Temporal cortex of 6 AD and 6 MCI patients and 11 non-demented controls	miR-107	down	BACE1	miRanda, TargetScan, PicTar, luciferase reporter assay	increased production of $A\beta$
Hébert et al., 2008 (16)	Anterior temporal cortex of 5 AD patients and 5 age-matched controls	miR-29a/b-1	down	BACE1	miRanda, TargetScan, PicTar, miRBase; luciferase reporter assay	increased production of $A\beta$
		miR-15a, miR-9, miR-19b	down	BACE1	miRanda, TargetScan, PicTar, miRBase; not validated	
		let-7i, miR-15a, miR-101, miR-106b	down	APP	miRanda, TargetScan, PicTar, miRBase; not validated	
		miR-22, miR-26b, miR-93, miR-181c, miR-210, miR-363	down	ND	ND	
		miR-197, miR-511, miR-320	up	ND	ND	

Authors, years, and reference No.	Brains of AD patients	MicroRNAs aberrantly expressed	Upregulation or downregulation	Target mRNAs characterized	Target prediction and validation	Possible pathological implications
Cogswell et al., 2008 (21)	Cerebellum of 15 AD patients and 12 non-demented controls	miR-27a, miR-27b, miR-34a, miR-100, miR-125b, miR-381, miR-422a	up	ND	miRanda, RNAhybrid	general neuropathology of AD
		miR-9, miR-98, miR-132, miR-146b, miR-212, miR-425	down	ARHGAP32 by miR-132		
	Hippocampus of 15 AD patients and 12 non-demented controls	miR-26a, miR-27a, miR-27b, miR-30e-5p, miR-34a, miR-92, miR-125b, miR-145, miR-200c, miR-381, miR-422a, miR-423	up	ND		
		miR-9, miR-30c, miR-132, miR-146b, miR-210, miR-212, miR-425	down	ARHGAP32 by miR-132		
	Medial frontal gyrus of 15 AD patients and 12 non-demented controls	miR-27a, miR-27b, miR-29a, miR-29b, miR-30c, miR-30e-5p, miR-34a, miR-92, miR-100, miR-125b, miR-145, miR-148a, miR-381, miR-422a, miR-423	up	ND		
	miR-9, miR-26a, miR-132, miR-146b, miR-200c, miR-210, miR-212, miR-425	down	ARHGAP32 for miR-132			
Hébert et al., 2009 (17)	Anterior temporal cortex of 19 AD patients and 11 non-demented controls	miR-106b	down	APP	miRanda, TargetScan, PicTar, miRBase; luciferase reporter assay	increased production of A $\beta$
Sethi and Lukiw, 2009 (14)	Temporal lobe cortex of 6 AD and 13 non-AD patients and 6 controls	miR-9, miR-125b, miR-146a	up	ND	ND	general neuropathology of AD
Nunez-Iglesias et al., 2010 (22)	Parietal lobe cortex of 5 AD patients and 5 age-matched controls	miR-18b, miR-34c, miR-615, miR-629, miR-637, miR-657, miR-661, mir-09369, mir-15903, mir-44691	ND	positively correlated with target mRNAs	miRanda, TargetScan, PicTar; not validated	general neuropathology of AD
		miR-211, miR-216, miR-325, miR-506, miR-515-3p, miR-612, miR-768-3p, mir-06164, mir-32339, mir-45496	ND	negatively correlated with target mRNAs	miRanda, TargetScan, PicTar; not validated	
Shioya et al., 2010 (23)	Frontal lobe of 7 AD patients and 4 non-neurological controls	miR-29a	down	NAV3	TargetScan, PicTar, miRBase; luciferase reporter assay	a putative compensatory mechanism against neurodegenerative events

AD, Alzheimer's disease; MCI, mild cognitive impairment; ND, not described; BACE1, beta-site APP-cleaving enzyme 1; APP, amyloid precursor protein; NAV3, neuron navigator 3; A $\beta$ , amyloid-beta; and ARHGAP32, Rho GTPase activating protein 32 (p250GAP).

29a/b-1 cluster, which inversely correlated with BACE1 protein levels, in the anterior temporal cortex of AD (16). The database search on miRanda, TargetScan, PicTar, and miRBase (MicroCosm) predicted the presence of several binding sites in the human BACE1 3'UTR for miR-9, miR-15a, miR-19b, and miR-29a/b-1 and in the human APP 3'UTR for let-7, miR-15a, miR-101, and miR-106b, all of which are downregulated in AD brains. They validated miR-29a-mediated downregulation of

BACE1 by the luciferase reporter assay. Furthermore, an introduction of the miR-29a/29b-1 precursors reduced secretion of A $\beta$  from HEK293 cells stably expressing APP Swedish (APPswe) (16). Subsequently, the same group reported reduced expression of miR-106b capable of targeting APP in the anterior temporal cortex of AD, although they did not find a clear-cut inverse correlation between the levels of miR-106b and APP protein expression (17).

Thus, different studies identified various miRNAs in AD brains. This variability is in part attributable to disease-specific and nonspecific interindividual differences, including differences in age, sex, the brain region, the pathological stage, and the postmortem interval (PMI), since most studies are performed on a fairly small number of samples and controls, complicated by variable confounding factors (Table 1). With respect to animal models of AD, a recent study showed that the expression levels of a noncoding BACE1-antisense (BACE1-AS) RNA that enhances BACE1 mRNA stability are elevated in the brains of Tg19959 APP transgenic mice and those of AD (18). Furthermore, the levels of miR-298 and miR-328, both of which reduce the expression of mouse BACE1 protein, are decreased in the hippocampus of aged APPswe/PS1 transgenic mice (19). All of these observations suggest that abnormally reduced expression of a set of miRNAs accelerates A $\beta$  deposition via overproduction of BACE1, the enzyme and/or APP, the substrate in AD brains. It is worthy to note that genetic variability involving miRNA-binding sites in both BACE1 and APP 3'UTRs does not serve as a major risk factor for development of AD (20), suggesting that minor variations in miRNA-binding sequences do not play a central role in upregulation of BACE1 and APP in AD brains. These observations sound reasonable because miRNAs generally induce translational inhibition without requiring the perfect match in the binding sequences of target mRNAs.

By the TaqMan microRNA assay-based semi-quantitative RT-PCR method, a previous study intensively characterized miRNA expression profiles of the brains and CSF samples derived from AD patients and nondemented controls (21). They found that a wide variety of miRNAs are either upregulated or downregulated in specific regions of AD brains at defined pathological stages, and the levels of all miR-30 family members are coordinately elevated in CSF samples of AD. They predicted miRNA-binding sites of the targets and then identified a relevant biological pathway by the hypergeometric enrichment method named miRNAPath. As a result, the analysis identified a meaningful relationship between upregulated miRNAs and metabolic pathways in AD brains such as insulin signaling, glycolysis, and glycogen metabolism (21). By combining microarray-based miRNA expression profiling and transcriptome analysis of the brains of AD patients and age-matched control subjects, a recent study showed that the levels of various miRNAs are not only negatively but also positively correlated with those of the potential target mRNAs (22). The expression of miR-211 shows a negative correlation with mRNA levels of BACE1, RAB43, LMNA, MAP2K7, and TADA2L, whereas the expression of mir-

44691 has a positive correlation with mRNA levels of CYR61, CASR, POU3F2, GGPR68, DPF3, STK38, and BCL2L2 in AD brains, supporting the previous observations that certain miRNAs activate transcription and translation of targets (4, 5).

### 3. miR-29a decreased in AD brains targets NAV3

To identify miRNAs aberrantly expressed in the brains of human neurodegenerative diseases, we initially studied miRNA expression profiles of the frontal cortex of three amyotrophic lateral sclerosis (ALS) patients on a microarray containing 723 miRNAs (23). The human frontal cortex total RNA of a 79 year-old Caucasian man who died of bladder cancer (AM6810, Ambion) was utilized as a universal reference. The microarray data were filtered through the following stringent criteria, that is, the detection of all signals above the threshold, the reference signal value exceeding 100, and the fold change expressed as the signal of ALS divided by the signal of the universal reference greater than 5. After filtration, we identified only three miRNAs, including miR-29a, miR-29b, and miR-338-3p, as a group of miRNAs whose expression is substantially upregulated in all three ALS brains (23).

Next, we increased the number of the cases to validate microarray data by TaqMan microRNA assay-based quantitative real-time RT-PCR (qRT-PCR). They include four non-neurological controls (NC), six patients with ALS, seven with AD, and four with PD. Most importantly, all the brains were carefully evaluated by pathological examination of the corresponding paraffin sections, following the Braak staging system to characterize the stage of AD pathology (24). Although we observed a trend for upregulation of miR-29a expression levels in ALS versus NC, the difference did not reach statistical significance due to a great interindividual variation. However, unexpectedly, we found that miR-29a expression levels were significantly reduced in AD when compared with NC ( $P = 0.041$ ) (Fig. 1a). On the other hand, the levels of miR-338-3p were not significantly different among the study groups, although a larger cohort is required to obtain a statistical power enough to make a definitive conclusion (23). Since miR-29a and miR-29b are located on the identical MIRN29B/MIRN29A gene cluster on chromosome 7q32.3, their biological functions are presumably similar. Therefore, we further focused our attention solely on miR-29a.

Then, we explored putative miR-29a target genes by searching them on web-accessible microRNA target databases, including TargetScan, PicTar, and miRBase (MicroCosm). When the top 200 most reliable miR-29a targets were extracted by each program, we found 11

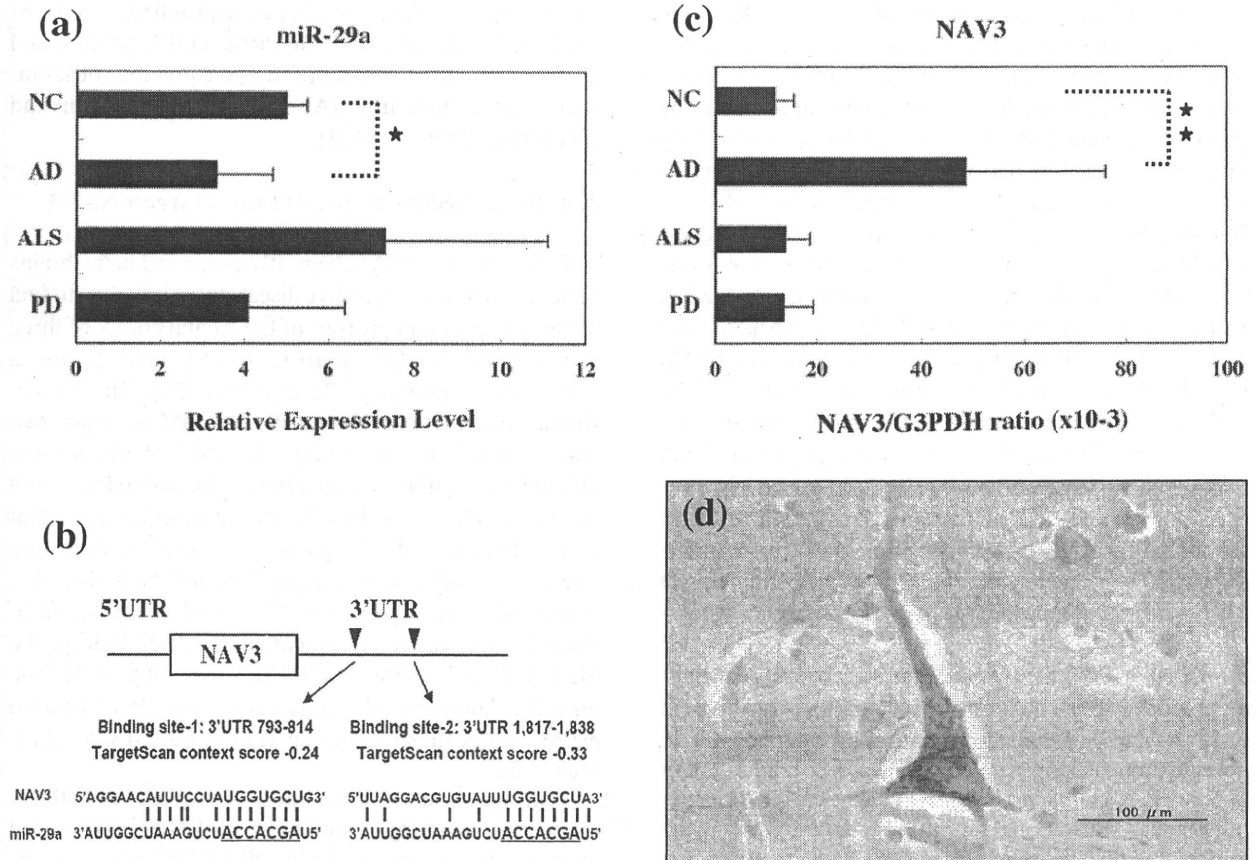


**Fig. 1.** MicroRNA-29a decreased in AD brain targets NAV3. a) qRT-PCR of miR-29a expression. The expression of miR-29a was studied in frozen frontal cortex tissues of non-neurological controls (NC) (n = 4), Alzheimer's disease (AD) (n = 7), amyotrophic lateral sclerosis (ALS) (n = 6), and Parkinson disease (PD) (n = 4) by TaqMan microRNA assay-based quantitative RT-PCR (qRT-PCR) following the Delta-Delta Ct method. RNU6B was utilized for an endogenous reference to standardize miRNA expression levels. The results were expressed as relative expression levels after calibration with the universal reference (AM6810, Ambion) data. The star indicates  $P = 0.041$  by Student's  $t$ -test. b) Two miR-29a-binding sites located in 3'UTR of the NAV3 gene. The 3'UTR of the human NAV3 gene contains two separate, evolutionarily conserved miR-29a-binding sites, located in the nucleotide positions 793 – 814 and 1,817 – 1,838. The seeding sequence of miR-29a is underlined. c) qRT-PCR of NAV3 mRNA expression. The expression of NAV3 mRNA was studied in frozen frontal cortex tissues of NC (n = 4), AD (n = 7), ALS (n = 6), and PD (n = 4) by qRT-PCR. The levels of NAV3 mRNA are standardized against those of G3PDH mRNA detected in identical cDNA samples. The double stars indicate  $P = 0.028$  by Student's  $t$ -test. d) Enhanced NAV3 immunoreactivity in degenerating pyramidal neurons in AD brains. The expression of NAV3 was studied in the frontal cortex tissue sections of AD by immunohistochemistry using anti-NAV3 antibody (ab69868, Abcam).

genes shared among the three programs: fibrillin 1 (FBN1); neuron navigator 3 (NAV3); collagen, type V, alpha 3 (COL5A3); collagen, type XI, alpha 1 (COL11A1); collagen, type I, alpha 2 (COL1A2); nuclear autoantigenic sperm protein (NASP); tripartite motif-containing 37 (TRIM37); post-GPI attachment to proteins 2 (PGAP2); collagen, type VI, alpha 3 (COL6A3); inducible T-cell co-stimulator (ICOS); and mediator complex subunit 12-like (MED12L) (23). Among them, NAV3, alternatively named pore membrane and/or filament interacting like protein 1 (POMFIL1), was selected for

further investigations because it is predominantly expressed in the nervous system (25). Although the precise biological function of NAV3 in the human brain remains unknown, a *Caenorhabditis elegans* gene named unc-53, highly homologous to NAV3, plays a key role in axon guidance (26). Although a previous study identified BACE1 as the most important target of miR-29a (16), we found BACE1 as one of miR-29a targets ranking 750th of 850 candidates on TargetScan and 197th of 326 candidates on PicTar.

The TargetScan search indicated that the 3'UTR of the

human NAV3 gene contains two separate miR-29a-binding sequences, highly conserved through evolution, located in the nucleotide positions 793–814 and 1,817–1,838 (Fig. 1b). We cloned the former in the luciferase reporter vector, which was cotransfected with a miR-29a expression vector in HEK293 cells. The expression of miR-29a significantly suppressed activation of the luciferase reporter following the wild-type target sequence, whereas miR-29a did not affect the expression of the reporter following the target sequence with a 6-bp deletion corresponding to the seed sequence (23). Importantly, qRT-PCR indicated that the levels of NAV3 mRNA expression were significantly higher in the frontal cortex of AD compared with NC ( $P = 0.028$ ) (Fig. 1c), suggesting that NAV3 is indeed a candidate for an miR-29a target *in vivo* in AD brains. However, we could not validate elevation of NAV3 protein levels in AD brains by western blot analysis due to a great interindividual variation (23). The lack of the correlation between mRNA levels and protein abundance might be in part attributable to the complexity of brain tissues composed of various cellular constituents with differential expression of target proteins that affects the efficacy of purification, or alternatively to the differential stability and turnover of mRNA and protein via various post-transcriptional mechanisms, including the selective degradation of proteins by proteasome and autophagosome machineries in individual cells (27).

Finally, we investigated NAV3 expression in the frontal cortex of AD, ALS, or PD by immunohistochemistry. In all the brains examined, large and medium-sized pyramidal neurons in layers III and V of the cerebral cortex expressed NAV3 immunoreactivity located chiefly in the cytoplasm, axons, and dendrites (23). Notably, NAV3 immunolabeling was the most intense in neurons presenting with degenerating morphology in AD brains (Fig. 1d). In AD brains, a substantial population (<20%) of pyramidal neurons containing tau-immunolabeled NFT coexpressed intense NAV3 immunoreactivity. However, at present, it remains unknown whether enhanced expression of NAV3 in a subpopulation of cortical pyramidal neurons in AD brains reflects a pathogenic change or a compensatory mechanism against neurodegenerative events. A recent study by *in situ* hybridization (ISH) showed that each subpopulation of neurons in different cerebral cortical layers expresses a distinct set of miRNAs in the human transentorhinal cortex (TEX), and the expression pattern is greatly affected by AD pathology from the earliest stage of the disease (28).

In conclusion, increasing evidence indicates that aberrant expression of various miRNAs, both upregulated and downregulated species, plays an active role in the

pathological processes of AD (Table 1). A single miRNA has a great impact on the cellular function by mostly suppressing and occasionally activating numerous downstream mRNA targets. Therefore, even the small-scale turbulence occurring in the miRNA-mediated gene regulation affects various biological pathways involved in both neurodegeneration and neuroprotection in AD brains. We need to further elucidate the entire picture of the pathophysiological interaction among miRNAs, mRNAs, and proteins in AD brains.

### Acknowledgements

Human brain tissues were provided by Research Resource Network (RRN), Japan. The author thanks Drs. Kunimasa Arima, Tsuyoshi Ishida, and Yuko Saito for pathological evaluation of human brain tissues and Mao Shioya, Shinya Obayashi, and Hiroko Tabunoki for technical assistance. This work was supported by a research grant from the High-Tech Research Center Project, the Ministry of Education, Culture, Sports, Science, and Technology (MEXT), Japan (S0801043) and a grant from Research on Intractable Diseases, the Ministry of Health, Labour, and Welfare of Japan (H22-Nanchi-Ippan-136).

### References

- 1 Kosik KS. The neuronal microRNA system. *Nat Rev Neurosci*. 2006;7:911–920.
- 2 Selbach M, Schwanhäusser B, Thierfelder N, Fang Z, Khanin R, Rajewsky N. Widespread changes in protein synthesis induced by microRNAs. *Nature*. 2008;455:58–63.
- 3 Filipowicz W, Bhattacharyya SN, Sonenberg N. Mechanisms of post-transcriptional regulation by microRNAs: are the answers in sight? *Nat Rev Genet*. 2008;9:102–114.
- 4 Vasudevan S, Tong Y, Steitz JA. Switching from repression to activation: microRNAs can up-regulate translation. *Science*. 2007;318:1931–1934.
- 5 Place RF, Li LC, Pookot D, Noonan EJ, Dahiya R. MicroRNA-373 induces expression of genes with complementary promoter sequences. *Proc Natl Acad Sci U S A*. 2008;105:1608–1613.
- 6 Fineberg SK, Kosik KS, Davidson BL. MicroRNAs potentiate neural development. *Neuron*. 2009;64:303–309.
- 7 Schratz GM, Tuebing F, Nigh EA, Kane CG, Sabatini ME, Kiebler M, et al. A brain-specific microRNA regulates dendritic spine development. *Nature*. 2006;439:283–289.
- 8 Mellios N, Huang HS, Grigorenko A, Rogav E, Akbarian S. A set of differentially expressed miRNAs, including miR-30a-5p, act as post-transcriptional inhibitors of BDNF in prefrontal cortex. *Hum Mol Genet*. 2008;17:3030–3042.
- 9 Nelson PT, Wang WX, Rajeev BW. MicroRNAs (miRNAs) in neurodegenerative diseases. *Brain Pathol*. 2008;18:130–138.
- 10 Kocerha J, Kauppinen S, Wahlestedt C. microRNAs in CNS Disorders. *Neuromolecular Med* 2009;11:162–172.
- 11 Serretti A, Olgiati P, De Ronchi D. Genetics of Alzheimer's disease. A rapidly evolving field. *J Alzheimers Dis*. 2007;12:73–92.
- 12 Lukiw WJ. Micro-RNA speciation in fetal, adult and Alzheimer's disease hippocampus. *Neuroreport*. 2007;18:297–300.
- 13 Lukiw WJ, Zhao Y, Cui JG. An NF- $\kappa$ B-sensitive micro RNA-

- 146a-mediated inflammatory circuit in Alzheimer disease and in stressed human brain cells. *J Biol Chem.* 2008;283:31315–31322.
- 14 Sethi P, Lukiw WJ. Micro-RNA abundance and stability in human brain: specific alterations in Alzheimer's disease temporal lobe neocortex. *Neurosci Lett.* 2009;459:100–104.
- 15 Wang WX, Rajeev BW, Stromberg AJ, Ren N, Tang G, Huang Q, et al. The expression of microRNA miR-107 decreases early in Alzheimer's disease and may accelerate disease progression through regulation of  $\beta$ -site amyloid precursor protein-cleaving enzyme 1. *J Neurosci.* 2008;28:1213–1223.
- 16 Hébert SS, Horré K, Nicolaï L, Papadopoulou AS, Mandemakers W, Silahatoglu AN, et al. Loss of microRNA cluster miR-29a/b-1 in sporadic Alzheimer's disease correlates with increased BACE1/beta-secretase expression. *Proc Natl Acad Sci U S A.* 2008;105:6415–6420.
- 17 Hébert SS, Horré K, Nicolaï L, Bergmans B, Papadopoulou AS, Delacourte A, et al. MicroRNA regulation of Alzheimer's amyloid precursor protein expression. *Neurobiol Dis.* 2009;33:422–428.
- 18 Faghihi MA, Modarresi F, Khalil AM, Wood DE, Sahagan BG, Morgan TE, et al. Expression of a noncoding RNA is elevated in Alzheimer's disease and drives rapid feed-forward regulation of  $\beta$ -secretase. *Nat Med.* 2008;14:723–730.
- 19 Boissonneault V, Plante I, Rivest S, Provost P. MicroRNA-298 and microRNA-328 regulate expression of mouse  $\beta$ -amyloid precursor protein-converting enzyme 1. *J Biol Chem.* 2009;284:1971–1981.
- 20 Bettens K, Brouwers N, Engelborghs S, Van Mieghroet H, De Deyn PP, Theuns J, et al. APP and BACE1 miRNA genetic variability has no major role in risk for Alzheimer disease. *Hum Mutat.* 2009;30:1207–1213.
- 21 Cogswell JP, Ward J, Taylor IA, Waters M, Shi Y, Cannon B, et al. Identification of miRNA changes in Alzheimer's disease brain and CSF yields putative biomarkers and insights into disease pathways. *J Alzheimers Dis.* 2008;14:27–41.
- 22 Nunez-Iglesias J, Liu CC, Morgan TE, Finch CE, Zhou XJ. Joint genome-wide profiling of miRNA and mRNA expression in Alzheimer's disease cortex reveals altered miRNA regulation. *PLoS One.* 2010;5:e8898.
- 23 Shioya M, Obayashi S, Tabunoki H, Arima K, Saito Y, Ishida T, et al. Aberrant microRNA expression in the brains of neurodegenerative diseases: miR-29a decreased in Alzheimer disease brains targets neuron navigator-3. *Neuropathol Appl Neurobiol.* 2010;36:320–330.
- 24 Braak H, Alafuzoff I, Arzberger T, Kretschmar H, Del Tredici K. Staging of Alzheimer disease-associated neurofibrillary pathology using paraffin sections and immunocytochemistry. *Acta Neuropathol.* 2006;112:389–404.
- 25 Coy JF, Wiemann S, Bechmann I, Bächner D, Nitsch R, Kretz O, et al. Pore membrane and/or filament interacting like protein 1 (POMFIL1) is predominantly expressed in the nervous system and encodes different protein isoforms. *Gene.* 2002;290:73–94.
- 26 Maes T, Barceló A, Buesa C. Neuron navigator: a human gene family with homology to unc-53, a cell guidance gene from *Caenorhabditis elegans*. *Genomics* 2002;80:21–30.
- 27 Laloo B, Simon D, Veilla V, Lauzel D, Guyonnet-Duperat V, Moreau-Gaudry F, et al. Analysis of post-transcriptional regulations by a functional, integrated, and quantitative method. *Mol Cell Proteomics.* 2009;8:1777–1788.
- 28 Nelson PT, Dimayuga J, Wilfred BR. MicroRNA in situ hybridization in the human entorhinal and transentorhinal cortex. *Front Hum Neurosci.* 2010;4:7.

## Original Article

# Immunohistochemical characterization of microglia in Nasu-Hakola disease brains

Jun-ichi Satoh,<sup>1</sup> Hiroko Tabunoki,<sup>1</sup> Tsuyoshi Ishida,<sup>2</sup> Saburo Yagishita,<sup>3</sup> Kenji Jinnai,<sup>4</sup>  
Naonobu Futamura,<sup>4</sup> Michio Kobayashi,<sup>5</sup> Itaru Toyoshima,<sup>6</sup> Toshiaki Yoshioka,<sup>7</sup>  
Katsuhiko Enomoto,<sup>7</sup> Nobutaka Arai<sup>8</sup> and Kunimasa Arima<sup>9</sup>

<sup>1</sup>Department of Bioinformatics and Molecular Neuropathology, Meiji Pharmaceutical University, <sup>8</sup>Department of Clinical Neuropathology, Tokyo Metropolitan Institute for Neuroscience, <sup>9</sup>Department of Psychiatry, National Center Hospital, NCNP, Tokyo, <sup>2</sup>Department of Pathology and Laboratory Medicine, Kohnodai Hospital, National Center for Global Health and Medicine, Chiba, <sup>3</sup>Department of Pathology, Kanagawa Rehabilitation Center, Kanagawa, <sup>4</sup>Department of Neurology, Hyogo-Cyuo National Hospital, Hyogo, <sup>5</sup>Department of Neurology, Akita National Hospital, <sup>6</sup>Department of Neurology and Medical Education Center, Akita University School of Medicine and <sup>7</sup>Department of Molecular Pathology and Tumor Pathology, Akita University School of Medicine, Akita, Japan

Nasu-Hakola disease (NHD) is a rare autosomal recessive disorder, characterized by progressive presenile dementia and formation of multifocal bone cysts, caused by genetic mutations of DNAX-activation protein 12 (DAP12) or triggering receptor expressed on myeloid cells 2 (TREM2). TREM2 and DAP12 constitute a receptor/adaptor signaling complex expressed on osteoclasts, dendritic cells (DC), macrophages and microglia. Previous studies using knock-out mice and mouse brain cell cultures suggest that a loss-of-function of DAP12/TREM2 in microglia plays a central role in the neuropathological manifestation of NHD. However, there exist no immunohistochemical studies that focus attention on microglia in NHD brains. To elucidate a role of microglia in the pathogenesis of NHD, we searched NHD-specific biomarkers and characterized their expression on microglia in NHD brains. Here, we identified allograft inflammatory factor 1 (AIF1, Iba1) and sialic acid binding Ig-like lectin 1 (SIGLEC1) as putative NHD-specific biomarkers by bioinformatics analysis of microarray data of NHD DC. We studied three NHD and eight control brains by immunohistochemistry with a panel of 16 antibodies, including those against Iba1 and SIGLEC1. We verified the absence of DAP12 expression in NHD brains and the expression of DAP12 immunoreactivity on

ramified microglia in control brains. Unexpectedly, TREM2 was not expressed on microglia but expressed on a small subset of intravascular monocytes/macrophages in control and NHD brains. In the cortex of NHD brains, we identified accumulation of numerous Iba1-positive microglia to an extent similar to control brains, while SIGLEC1 was undetectable on microglia in all the brains examined. These observations indicate that human microglia in brain tissues do not express TREM2 and DAP12-deficient microglia are preserved in NHD brains, suggesting that the loss of DAP12/TREM2 function in microglia might not be primarily responsible for the neuropathological phenotype of NHD.

**Key words:** bioinformatics, DAP12, microglia, Nasu-Hakola disease, TREM2.

## INTRODUCTION

Nasu-Hakola disease (NHD; OMIM 221770), also designated polycystic lipomembranous osteodysplasia with sclerosing leukoencephalopathy (PLOS), is a rare autosomal recessive disorder, characterized by progressive presenile dementia and formation of multifocal bone cysts filled with convoluted adipocyte membranes.<sup>1,2</sup> The clinical course of NHD is classified into four stages: (i) the latent stage with normal early development; (ii) the osseous stage beginning at the third decade of life, presenting with pain and swelling of ankles and feet followed by pathological bone fractures; (iii) the early neuropsychiatric stage occurring at the fourth decade of life, presenting with a frontal lobe syndrome such

Correspondence: Jun-ichi Satoh, MD, Department of Bioinformatics and Molecular Neuropathology, Meiji Pharmaceutical University, 2-522-1 Noshio, Kiyose, Tokyo 204-8588, Japan. Email: satoji@my-pharm.ac.jp

Received 23 July 2010; revised and accepted 27 September 2010.



as euphoria and loss of social inhibitions; and (iv) the late neuropsychiatric stage, presenting with profound dementia, loss of mobility and death usually by age 50 years.<sup>3</sup> The neuropathological hallmark of NHD includes profound loss of myelin and axons, and accumulation of axonal spheroids and sudanophilic granules, accompanied by intense astrogliosis predominantly in the frontal and temporal lobes and the basal ganglia.<sup>4,5</sup>

Nasu-Hakola disease is caused by a structural defect in one of the two genes, DNAX-activation protein 12 (DAP12), alternatively named TYRO protein tyrosine kinase-binding protein (TYROBP) on chromosome 19q13.1, or triggering receptor expressed on myeloid cells 2 (TREM2) on chromosome 6p21.1. Seventeen different NHD-causing loss-of-function mutations currently identified in either DAP12 or TREM2 cause an identical disease phenotype.<sup>6,7</sup> DAP12 is expressed as a disulfide-bonded homodimer on natural killer (NK) cells, monocytes/macrophages, dendritic cells (DC), osteoclasts, and brain microglia. DAP12 constitutes a transmembrane adaptor that noncovalently associates with several cell-surface receptors, including natural cytotoxicity triggering receptor 2 (NCR2), TREM2, TREM1, signal-regulatory protein beta 1 (SIRPB1), and myeloid DAP12-associating lectin 1 (MDL1), and transmits either activating or inhibitory signals depending on the avidity of their ligands.<sup>8</sup> DAP12-deficient mice develop osteopetrosis, hypomyelinoses accentuated in the thalamus, and synaptic degeneration, suggesting that DAP12 signaling is essential for development of osteoclasts and oligodendrocytes and synaptogenesis.<sup>9</sup> DAP12-deficient macrophages produced higher concentrations of inflammatory cytokines in response to toll-like receptor (TLR) stimulation.<sup>10</sup> The synaptic function is altered in DAP12 loss-of-function mice due to reduced expression of AMPA receptor GluR2 subunit and TrkB.<sup>11</sup> Furthermore, the number of microglia is greatly reduced in the brain of DAP12-deficient/loss-of-function mice.<sup>12,13</sup>

TREM2 is expressed on osteoclasts, DC, macrophages and microglia, and recognizes polyanionic macromolecules, bacteria and heat shock protein HSP60.<sup>14-17</sup> Apoptotic neuronal cell membranes express endogenous TREM2 ligands.<sup>18</sup> Crosslinking of TREM2 on cultured mouse microglia triggers phagocytosis of apoptotic neurons without secretion of proinflammatory cytokines, while knockdown of TREM2 inhibits phagocytosis of apoptotic neurons and stimulates production of proinflammatory cytokines such as TNF and IL-1 $\beta$ .<sup>19</sup> These observations suggest the hypothesis that the pathogenesis of NHD is mainly attributable to the inability of DAP12/TREM2-deficient microglia to remove apoptotic neurons, followed by enhanced production of proinflammatory cytokines in the brain. However, at present, the precise role of microglia

in persistent demyelination, gliosis and axonal degeneration in NHD brains, caused by loss of function of DAP12/TREM2, remains largely unknown. There exist no immunohistochemical studies that focus attention on microglia in NHD brains.

To investigate an active role of microglia in the neuropathological manifestation of NHD, first we attempted to identify NHD-specific biomarker genes by *in silico* bioinformatics analysis of microarray data. Then, we studied three NHD brains, compared with eight control brains side by side, by immunohistochemistry using a panel of antibodies against cell type-specific markers and putative disease-specific biomarkers.

## MATERIALS AND METHODS

### Hierarchical clustering analysis of microarray data

The microarray dataset GSE3624 was downloaded from of the Gene Expression Omnibus (GEO) repository (<http://www.ncbi.nlm.nih.gov/geo>). In this dataset, RNA was prepared from peripheral blood monocyte-derived dendritic cells (DC) induced by IL-4 and GM-CSF isolated from three NHD patients with DAP12 mutation of EX1-4 DEL, two NHD patients with TREM2 mutation of either Q33X or V126G, and three normal control (NC) subjects.<sup>20</sup> The gene expression profile was analyzed by the Affymetrix Human Genome HG-U133A chip containing 22 283 transcripts, and the data were normalized following the Microarray Analysis Suite 5.0 (MAS5: Affymetrix, Santa Clara, CA, USA) algorithm. To identify NHD DC-specific biomarker genes, we selected 226 differentially expressed genes (DEGs) by comparing the transcriptome data among DAP12-mutated patients, TREM2-mutated patients, and NC subjects with one-way analysis of variance (ANOVA) ( $P < 0.001$ ). Among them, we extracted 73 DEGs showing the changes in expression levels greater than 2-fold or smaller than 0.5-fold in DAP12-mutated patients versus NC subjects, after omitting the genes called as absent (A) or marginal (M). Then, these data were imported into the Cluster 3.0 software ([bonsai.ims.u-tokyo.ac.jp/~mdehoon/software/cluster](http://bonsai.ims.u-tokyo.ac.jp/~mdehoon/software/cluster)), followed by visualizing them on Java TreeView1.1.3 ([sourceforge.net/projects/jtreeview](http://sourceforge.net/projects/jtreeview)).

### Molecular network analysis

Ingenuity Pathways Analysis (IPA) 8.5 is a knowledgebase that contains approximately 2 270 000 biological and chemical interactions and functional annotations with scientific evidence. They are collected from more than 500 selected articles, textbooks and other data sources, manu-

**Table 1** Primary antibodies utilized for immunohistochemistry

Antibody	Supplier	Code (ID)	Origin	Antigen	Concentration
DAP12	Santa Cruz Biotechnology	sc-20783 (FL-113)	Rabbit	Full-length human DAP12 protein	1:500
TREM2	Sigma	HPA010917	Rabbit	A peptide composed of AAWHGQKPGTHPPSELDCG HDPGYQLQTLPLGRDT	1:100
TREM1	Sigma	HPA005563	Rabbit	A peptide composed of PGSNENSTQNVYKIPPTTTKAL CPLYTSPRTVTQAPPKSTADVS TPDSEINLTNVTDI	1:250
IBA1	Wako	019-19741	Rabbit	A synthetic peptide corresponding to the C-terminus of Iba1	1:2000
HLA-DR	Dako	M0746 (TAL.1B5)	Mouse	The $\alpha$ -chain subunit of HLA class II DR antigens	1:100
CD68	Dako	N1577 (KP1)	Mouse	Lysosomal granules of human lung macrophages	Prediluted
CD163	Novocastra	NCL-CD163 (10D6)	Mouse	Recombinant human CD163 protein corresponding to domains of 1 to 4 of the N-terminal region	1:50 of the hybridoma culture supernatant
MSR1	Transgenic	KT022 (SRA-E5)	Mouse	Recombinant human MSR1 (CD204) protein	1:100
SIGLEC1	Santa Cruz Biotechnology	sc-53442 (HSn7D2)	Mouse	Fc fusion protein containing N-terminal 4 domains of human Siglec1	1:20
SIRPB1	Proteintech Group	11811-1-AP	Rabbit	Recombinant human SIRBP1 protein	1:1000
GFAP	Dako	N1506	Rabbit	GFAP purified from bovine spinal cord	Prediluted
MBP	Dako	N1564	Rabbit	MBP purified from human brain	Prediluted
NF	Nichirei	412551 (2F11)	Mouse	NF purified from human brain	Prediluted
SYNAP	Novocastra	NCL-SYNAP-299 (27G12)	Mouse	A synthetic peptide corresponding to the region close to the C-terminus of synaptophysin	1:500 of the hybridoma culture supernatant
CD3	Nichirei	413241 (PS1)	Mouse	Recombinant human CD3 epsilon chain protein	Prediluted
Cleaved Caspase-3	Cell Signaling Technology	#9661 (Asp175)	Rabbit	A peptide mapping amino-terminal residues adjacent to Asp175 of human caspase-3	1:100

GFAP, glial fibrillary acidic protein; MBP, myelin basic protein; MSR1, macrophage scavenger receptor 1; NF, neurofilament protein; SIGLEC1, sialic acid binding Ig-like lectin 1; SIRPB1, signal-regulatory protein beta 1; SYNAP, synaptophysin; HLA-DR, human leukocyte antigen MHC class II DR.

ally curated by expert biologists. By uploading the gene list, the network-generation algorithm identifies focused genes integrated in a global molecular network.<sup>21</sup> IPA calculates the *P*-value, the statistical significance of association between the genes and the network by Fisher's exact test.

### Human brain tissues

The brain tissues were obtained from Research Resource Network (RRN), Tokyo, Japan. Written informed consent at autopsy was obtained for all cases, following the regulations of the institutional ethics committees. The present study includes three patients with NHD, composed of a 42-year-old man (NHD1), a 48-year-old woman (NHD2), and a 44-year-old man (NHD3), four patients with myotonic dystrophy (MD) selected as neurological disease con-

trols, composed of a 68-year-old man (MD1), a 61-year-old man (MD2), a 60-year-old man (MD3) and a 53-year-old woman (MD4), and four subjects who died of non-neurological causes (NC), composed of a 63-year-old man who died of prostate cancer and acute myocardial infarction (NC1), a 67-year-old man who died of dissecting aortic aneurysm (NC2), a 57-year-old man who died of alcoholic liver cirrhosis (NC3) and a 61-year-old man who died of rheumatoid arthritis with interstitial pneumonia (NC4). The brain regions include the frontal cortex, the hippocampus and the basal ganglia in NHD cases, and the frontal cortex and the hippocampus in MD and NC cases. The homozygous mutation of a single base deletion of 141G (141delG) in exon 3 of DAP12 was identified in NHD1 and NHD2, while the genetic analysis was not performed in NHD3.

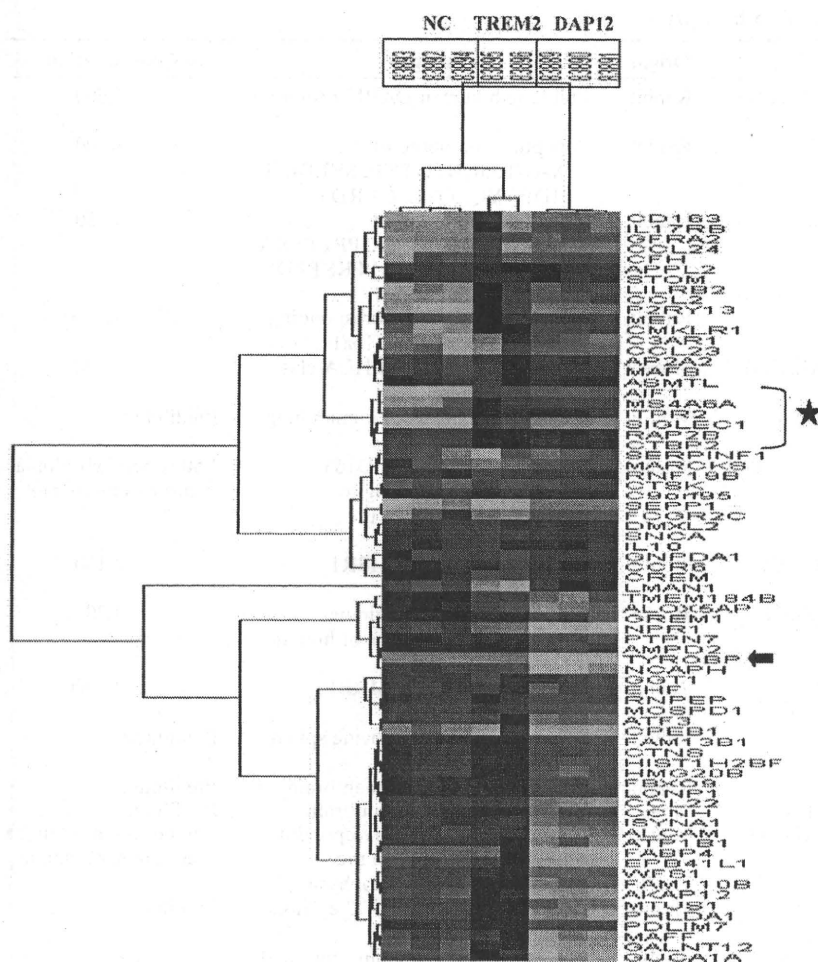


**Fig. 1** Hierarchical clustering analysis of transcriptome data of dendritic cells isolated from Nasu-Hakola disease (NHD) patients. The dataset GSE3624 is composed of genome-wide transcriptome data of dendritic cells (DC) isolated from three DNAX-activation protein 12 (DAP12)-mutated patients, two triggering receptors expressed on myeloid cells 2 (TREM2)-mutated patients, and three normal control (NC) subjects. By bioinformatics analysis of this dataset, we identified 73 genes differentially expressed in DC of DAP12-mutated patients. They were processed for hierarchical clustering analysis. In the heat map, red and green colors represent upregulation or downregulation, respectively. TYROBP (DAP12) is indicated by an arrow. Six NHD-specific biomarker candidates (AIF1, MS4A6A, ITPR2, SIGLEC1, RAP2B and CTBP2) are bracketed by a star.

## Immunohistochemistry

After deparaffination, tissue sections were heated in 10 mmol/L citrate sodium buffer by autoclave at 125°C for 30 s in a temperature-controlled pressure chamber (Dako, Tokyo, Japan). They were exposed to 3% hydrogen peroxide-containing methanol at room temperature (RT) for 15 min to block the endogenous peroxidase activity. The tissue sections were then incubated with PBS containing 10% normal goat serum at RT for 15 min to block non-specific staining. They were incubated in a moist chamber at 4°C overnight with primary antibodies listed in Table 1. Among the primary antibodies utilized, we validated the specificity of anti-TREM2 antibody and anti-DAP12 antibody by Western blot analysis of protein extract of HEK293 cells expressing corresponding recombinant proteins. After washing with PBS, the tissue sections were labeled at RT for 30 min with a horseradish peroxidase (HRP)-conjugated secondary antibody (Nichirei, Tokyo, Japan), followed by incubation with a colorizing solution containing diaminobenzidine tetrahydrochloride

(DAB). For double immunolabeling, the incubation of primary antibodies was followed by incubation with alkaline phosphatase (AP)-conjugated secondary antibody (Nichirei), and colorized with New Fuchsin substrate. All the sections were exposed to a counterstain with hematoxylin. For negative controls, the step of incubation with primary antibodies was omitted.

## RESULTS

### Bioinformatics approach identified molecular biomarkers and networks in DC of NHD

The dataset GSE3624 is composed of genome-wide transcriptome data of peripheral blood monocyte-derived DC expanded *in vitro* isolated from three DAP12-mutated patients, two TREM2-mutated patients and three NC subjects.<sup>20</sup> By reanalyzing the dataset with one-way ANOVA, we identified 226 differentially expressed genes (DEGs) among DAP12-mutated, TREM2-mutated and NC groups.

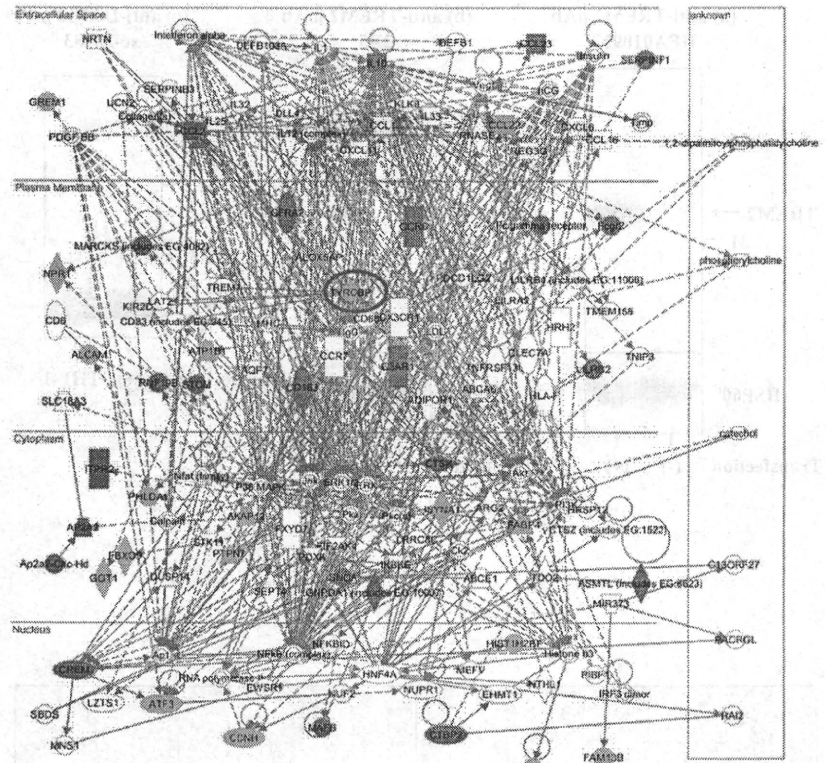


**Fig. 2** Molecular network of 73 genes differentially expressed in dendritic cells of DNAX-activation protein 12 (DAP12)-mutated patients. The molecular network of 73 genes differentially expressed in dendritic cells (DC) of DAP12-mutated patients was analyzed by Ingenuity Pathways Analysis (IPA). It constitutes a highly complex network that has the most significant relationship with inflammatory response, cell signaling, and molecular transport. Red and green nodes represent upregulated or down-regulated genes, respectively. TYROBP (DAP12) is enclosed by a blue circle.

From these, we extracted 73 DEGs, either upregulated or downregulated in DAP12-mutated patients. Hierarchical clustering analysis of 73 DEGs produced a heat map showing that the expression of TYROBP (DAP12) was greatly reduced in DC of DAP12-mutated patients, while it was preserved in those of TREM2-mutated patients and NC subjects (Fig. 1, arrow). Importantly, a panel of genes composed of allograft inflammatory factor 1 (AIF1), alternatively named ionized calcium-binding adapter molecule 1 (Iba1), membrane-spanning 4-domains, subfamily A, member 6A (MS4A6A), inositol 1,4,5-triphosphate receptor, type 2 (ITPR2), sialic acid binding Ig-like lectin 1 (SIGLEC1), RAP2B, member of RAS oncogene family (RAP2B), and C-terminal binding protein 2 (CTBP2) were upregulated in DC of both DAP12-mutated and TREM2-mutated patients compared with NC subjects, suggesting that the six genes represent a candidate for NHD-specific biomarker molecules (Fig. 1, star). Because previous studies reported that microglia express Iba1 and SIGLEC1,<sup>22,23</sup> we selected both for immunohistochemical analysis.

The molecular network analysis of 73 DEGs by IPA showed a highly complex network that has the most significant relationship with inflammatory response, cell signaling, and molecular transport ( $P = 1.00E-67$ ), suggesting that aberrantly expressed genes in DAP12-mutated DC

involve dysregulation of a wide range of inflammatory signaling events (Fig. 2).

### Preservation of microglia in the brains of NHD

We studied the tissue section of the frontal cortex, the hippocampus, the basal ganglia and surrounding regions of three NHD patients by immunohistochemistry, using a panel of 16 antibodies (Table 1). The specificity of anti-TREM2 antibody (HPA010917) and anti-DAP12 antibody (sc-20783) utilized in the present study was carefully validated by Western blot analysis of protein extract derived from HEK293 cells expressing recombinant human TREM2 or DAP12 protein (Fig. 3a-c). Previous studies showed that both DAP12 and TREM2 are expressed predominantly in microglia in the normal human and mouse CNS.<sup>14-16</sup> In control brains, we identified DAP12 immunoreactivity on the majority of ramified microglia (Fig. 4a) and an extremely small subset of cortical neurons but not on oligodendrocytes, whereas no DAP12-immunoreactive cells were detectable in NHD brains (Fig. 4b). Unexpectedly, TREM2 was not expressed on microglia but found on a small population of intravascular monocytes/macrophages and an extremely small subset of cortical neurons in control and NHD brains (Fig. 4c,d).